FedRME: Federated Learning for Enhanced Distributed Radiomap Estimation

Weishan Zhang*, Yue Wang†, Lingjia Liu‡, Zhi Tian*
*Department of Electrical and Computer Engineering, George Mason University, Fairfax, VA, USA
†Department of Computer Science, Georgia State University, Atlanta, GA, USA
‡Department of Electrical and Computer Engineering, Virginia Tech, Blacksburg, VA, USA
Emails: wzhang23@gmu.edu, ywang182@gsu.edu, ljliu@vt.edu, ztian1@gmu.edu

***Abstract*—For future intelligent communication systems, radiomap estimation (RME) is essential for acquiring panoramic awareness of spectrum spatial distribution in wireless environments. Recently, deep learning-based RME methods have been developed to reconstruct radiomaps from spectrum measurements collected at distributed sensors. However, these methods rely on gathering all input data at a central fusion center, resulting in large communication overheads, high computation costs, and privacy leakage concerns. To address these challenges, this work proposes a FedRME approach that makes federated learning applicable for distributed RME over a large-scale network, accommodating geographically heterogeneous transmitter locations and propagation environments. Specifically, we partition the large area into smaller regions to reduce the model complexity required for learning the radiomap in each region. Meanwhile, we incorporate the landscape map as an auxiliary input to induce a common learning model that adheres to the same propagation physics across all these heterogeneous regions. In doing so, fusion centers in all regions can collaborate through federated learning to enhance the overall RME performance. Simulation results indicate that our proposed method outperforms existing benchmarks, particularly under limited data, achieving higher learning accuracy with reduced model complexity and lower computational cost.**

***Index Terms*—Radiomap estimation, spectrum cartography, cognitive radio, distributed learning, federated learning.**

I. Introduction

Radiomap estimation (RME) plays as a tool for gaining awareness of spectrum coverage and environment, which is essential for dynamic spectrum access and intelligent spectrum management in next-generation wireless communication systems [1]. RME aims at mapping the distribution of radio signal strength or power in a given spatial domain, from spectrum measurements collected at distributed sensors [2]–[13]. Conventionally, RME is conducted through interpolation algorithms like compressive sensing [2], kriging [3], dictionary learning [4], matrix completion [5], and Bayesian models [6]. These methods fail to work effectively in real world, due to their inability to capture the complex channel characteristic of wireless networks [7]. Recently, data-driven deep learning methods have been introduced to enhance the performance of RME, especially in complex wireless environments [7]–[14]. These methods leverage the learning power of deep neural network (DNN) models from large volumes of training data, to learn the characteristics of the radio propagation environments and reconstruct the fine-resolution dense radiomaps from observations.

To the best of our knowledge, most existing learning-based RME methods are applied in a centralized manner. It inevitably requires all sensors distributed in the target area to timely transmit spectrum measurements collected in their locations to a central fusion center [7]–[12]. However, such global data collection by a single fusion center is not realistic for large-scale wireless scenarios. The large spatial region of the target area prevents centralized learning methods from practical implementation, due to their high communication and computation costs. Because the central fusion center processes all the data collected from (remote) sensors, it has to deal with a very large input dimensionality corresponding to the entire monitoring area, which hinges on a huge DNN model. On the other hand, the scarcity of training data, as a common issue in deep learning for wireless communications, triggers the notorious overfitting problem in the centralized RME methods. This is because the centralized RME has to train a large model with high-dimensional inputs using limited training data.

To address the aforementioned challenges, we propose a distributed RME framework named FedRME based on federated learning [15], with our contributions listed as follows. (i) For RME over a large geographical area, we first partition the large area into smaller regions, each served by a local fusion center. While these fusion centers are collaborative, each individually estimates the radiomap within its small region, allowing for the use of a compact learning model. (ii) Given the heterogeneity of these small regions due to varying transmitter locations and propagation environments, we incorporate the landscape map as an auxiliary input to induce a common learning model for all regions. The underlying principle is that all measurement data adhere to the same propagation physics, even though the local models account for regional difference in input. This consistency allows the use of a shared compact model for local RME across all regions. We then design federated learning solutions to enable distributed fusion centers in different regions to collaborate, thereby enhancing learning accuracy and overall RME performance. (iii) We evaluate the proposed FedRME through experimental simulations, where our FedRME outperforms the centralized benchmark and the

This work was supported in part by the National Science Foundation grants #1939553, #2128594, #2128596, #2231209, and #2413622.

standalone method in terms of higher RME learning accuracy.

II. Problem Statement

This section formulates the problem of RME in which the received signal strength across spatial and frequency domains is estimated using spectrum measurements collected from distributed sensors. We start with the signal model and then formulate the RME problems under two scenarios: centralized RME using a single global fusion center, and distributed RME using multiple distributed local fusion centers.

A. Spatial distribution of received signal strength

Consider a large target area under monitoring, which, without loss of generality, is assumed to be rectangular shape and discretized into $I \times J$ uniformly spaced grids. Assume there are S transmitters present, and let $\Upsilon_s(f), s \in [S]$ denote the transmit power spectrum density (PSD) of the s-th transmitter at a finite set of frequencies $f \in \mathcal{F} = \{f_1, \ldots, f_{N_f}\}$. Let $H_s(i,j,f)$ represent the frequency response of the channel between the s-th transmitter and the location at grid (i,j). The radiomap $\mathbf{\Psi} \in \mathbb{R}^{I\times J\times N_f}$ is formulated as the distribution of the received PSD across all grids of the whole area:

$$\mathbf{\Psi}(i,j,f) = \sum_{s=1}^{S} \Upsilon_s(f)|H_s(i,j,f)|^2 + \upsilon(i,j,f), \qquad (1)$$

where $\upsilon(i,j,f)$ denotes the noise. The objective for RME is to calculate $\hat{\mathbf{\Psi}} \in \mathbb{R}^{I\times J\times N_f}$, an estimate of the received power distribution on all grid points across the target rectangle area. The RME performance is measured by the root mean square error (RMSE) between the ground truth and estimation:

$$\mathbf{RMSE} = \sqrt{\frac{\mathbb{E}\{||\mathbf{\Psi} - \hat{\mathbf{\Psi}}||_F^2\}}{IJN_f}} \qquad (2)$$

B. Radiomap estimation with centralized learning

For realistic RME scenarios where transmitter configurations, including their locations and transmission PSDs, are unavailable, RME is conducted given measurements collected by distributed sensors. Assuming there are N ($N \ll IJ$) sensors deployed in the target area, each collecting the PSD $\tilde{\mathbf{\Psi}}(\boldsymbol{x}_n, f)$ at its location $\boldsymbol{x}_n$. In the centralized scenario, measurements of all the N sensors in the target area are assembled in a central fusion center. The task of the fusion center is to train a deep learning model to generate $\hat{\mathbf{\Psi}}$ based on centralized measurements $\{(\boldsymbol{x}_n, \tilde{\mathbf{\Psi}}(\boldsymbol{x}_n, f)), n \in [N], f \in \mathcal{F}\}$.

C. Radiomap estimation with distributed fusion centers

In realistic scenarios, considering various concerns in centralized RME, e.g., communication cost, computation complexity, and privacy leakage, distributed fusion centers are preferred since each of them interacts with a small group of sensors nearby. Specifically, the whole area is evenly partitioned into $N_x \times N_y$ smaller patches, and each fusion center-$k, k \in [N_xN_y]$, is responsible to train a deep model for estimating patch-k of the entire radiomap:

$$\hat{\mathbf{\Psi}}_k = \hat{\mathbf{\Psi}}(I_k : I_k + \frac{I}{N_x}, J_k : J_k + \frac{J}{N_y}, f), \qquad (3)$$

where I_k and J_k are the starting row and the starting column of patch-k, respectively. To improve the RME accuracy of each distributed fusion center-k, we allow it to assemble sensor measurements from a slightly larger region than $\frac{I}{N_x} \times \frac{J}{N_y}$ grids in patch-k. Finally, the complete estimation of the target area, $\hat{\mathbf{\Psi}}$, is formed by combining the outputs of different fusion centers, as illustrated in Fig. 1.

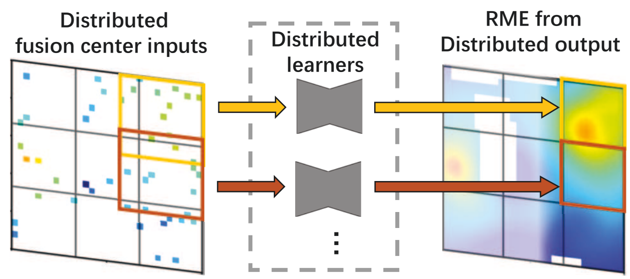

Fig. 1. Radiomap estimation with distributed fusion centers.

III. FedRME: distributed Radiomap Estimation

In this section, we develop a novel federated learning method for RME with distributed fusion centers. We start by introducing the overall design of our federated learning system. Then, we explain the convolutional autoencoder models that are used for reconstructing distributed radiomaps. Further, we describe the training scheme of our method.

A. Federated learning system for distributed RME

Due to heterogeneous building obstacles and transmitter deployment, which are dominating factors for signal propagation, the wireless environment varies among different patches of the whole area. The learning tasks of different fusion centers, based on their regional sensor data, is therefore heterogeneous. To address this issue, we include local landscape maps to the input, which contains core information about the building obstacles. In this way, distributed fusion centers can learn the impact of building obstacles under the same propagation physics. Based on this fact, we leverage the federated learning scheme to train a homogeneous deep model, by collaborative and efficient deep learning at distributed fusion centers.

To estimate the radiomap of the entire area, we set up a federated learning system that is composed of $K = N_xN_y$ distributed fusion centers. Assume fusion center-k collects input measurements from a wider range of grids than patch-k: $(I_k - d : I_k + \frac{I}{N_x} + d, J_k - d : J_k + \frac{J}{N_y} + d)$, with $d \ll min\{I,J\}$. Let set $\boldsymbol{N}_k$ denote the indices of sensors deployed in this range. To embed important auxiliary information including sensor locations and the propagation terrain, each fusion center-k generates input sample $\breve{\mathbf{\Psi}}_k$ by concatenating the local incomplete radiomap $\mathbf{\Psi}'_k$, the sensor location mask $\mathbf{M}_k$, and the landscape map $\mathbf{M}'_k$ [9]. The incomplete radiomap $\mathbf{\Psi}'_k$ contains sensor measurements $\{(\mathbf{x}_n, \tilde{\mathbf{\Psi}}(\mathbf{x}_n, f)), n \in \boldsymbol{N}_k\}$ assigned to their corresponding grids (i_n, j_n)'s and zero values otherwise. The sensor location mask $\mathbf{M}_k \in \mathbb{B}^{I\times J}$ is a binary matrix that utilizes the value "1" to indicate the grids that have sensor measurement assigned [16]–[18]. The landscape map $\mathbf{M}'_k \in \mathbb{B}^{I\times J}$ indicates the coverage of building obstacles in patch-k, which is highly impactful to wireless propagation. Given input sample $\breve{\mathbf{\Psi}}_k$, the distributed fusion center trains a deep learning model to generate $\hat{\mathbf{\Psi}}_k$. To avoid the need for external measurements outside the target area or zero-padding, fusion centers working on the outermost circle of the area generate their inputs by expanding the patch for $2d$ from their edges to the inner side.

The local training dataset of the j-th fusion center contains both the input measurement $\breve{\mathbf{\Psi}}_k$ and the ground truth radiomap of the corresponding expanded patch, e.g., $\mathbf{\Psi}(I_k - d : I_k + \frac{I}{N_x} + d, J_k - d : J_k + \frac{J}{N_y} + d)$. In this way, distributed fusion centers can collaboratively learn the common propagation physics in the area, especially the impact of obstacles, and apply it to local RME according to given landscape maps. For estimating the whole target area, all fusion centers should crop their outputs to the original size of $\frac{I}{N_x} \times \frac{J}{N_y}$ grids and stitch them together.

Meanwhile, by reducing the dimensionality of the radiomap estimated by each model, the complexity of estimating one patch by a distributed fusion center is significantly lower than estimating the whole area in the centralized method. The model complexity of distributed fusion centers can be reduced, leading to compact model design at realistic fusion center devices with limited hardware and computing resources.

B. Autoencoder model for distributed RME

We apply convolutional autoencoders for distributed fusion centers to reconstruct their relevant patches of the target map. The autoencoder deep neural network (DNN) is a concatenation of an encoder and a decoder [19]. The encoder is supposed to extract low-dimensional key information from the input, which is regarded as the "code" or latent variable. For conventional autoencoders, the decoder is supposed to reconstruct the input variable given the "code". For this purpose, autoencoders can be trained in an unsupervised manner, where the original input is also the label.

For radiomap estimation, the input variable $\breve{\mathbf{\Psi}}_k$ contains the incomplete radiomap as well as the sensor locations and the landscape map. The first task of the encoder network is to extract key information about the transmitters' locations and emission powers. The second task is to learn the key features of the landscape map. Both types of information are merged into the latent variable, which is the input to the decoder. In this sense, if the distributed fusion center collects data from enough distributed sensors, the incomplete radiomap input can provide sufficient information about the transmitters. Meanwhile, the code length of the latent variable should also be large enough to deliver this information to the decoder.

Another important factor for accurate RME is the learning capability of the encoder and decoder. We develop our autoencoder model as a fully convolutional structure. The learning architectures of the encoder network are convolutional layers. The rationale for utilizing convolutional filtering includes: (i) it can significantly reduce the volume of model parameters compared with fully connected layers, (ii) it is effective in capturing 2-D structure in radiomaps, which reflects the geographical distribution of signal strength, and (iii) it possesses the property of shift-invariance, which is suitable for learning the propagation phenomenon. The dimensionality of the feature map during the encoding process is reduced by several average pooling layers. The encoder design is shown in Fig. 2.

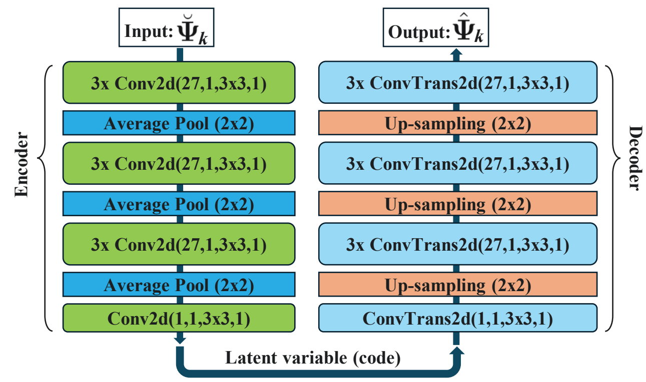

Fig. 2. Autoencoder design for centralized radiomap estimation.

The architecture of the decoder network resembles that of the encoder, which is also shown in Fig. 2. Specifically, the convolutional layers are replaced by convolution transpose layers, also known as "deconvolutional" layers. Similarly, the average pooling layers are replaced with up-sampling layers with bilinear interpolation, which gradually increases the dimensionality of feature maps until they match the input.

C. Federated learning scheme

The training scheme of our FedRME consists of two iterative stages: local training and parameter averaging. For parameter averaging, we assign a central parameter server to coordinate and aggregate local models among all fusion centers. Details for training are explained as follows.

Local training: For the k-th fusion center, the parameters of its autoencoder, denoted as W^k, are trained with its locally available data $\mathcal{D}_k$. Here, these local autoencoders are updated to minimize the mean square error loss function between the ground truth and the estimated radiomap of the corresponding patch.

Parameter averaging: After the above local training phases at fusion centers are periodically completed, the trained parameters of local autoencoder models, W^k, need to be aggregated through parameter averaging and then broadcasted to distributed fusion centers. Thus, the parameter averaging between J fusion centers are conducted as:

$$\mathcal{W} = \frac{1}{K}\sum_{k=1}^{K} \mathcal{W}^k. \tag{4}$$

Our FedRME is implemented in Algorithm 1.

Algorithm 1 Federated training of distributed fusion centers.

Initialize $\mathcal{W}^k, k = 1, \dots, K$
for each round $m = 1, 2, \dots, M$ **do**
  for each user-k, $k = 1, \dots, K$ in parallel **do**
    $\mathcal{W}^k \leftarrow$ *Local training* via ADAM $(\mathcal{W}^k, \mathcal{D}_k)$
  end for
  Parameter averaging via (4):
end for

IV. Simulation Results

In this section, we present the simulation results to evaluate the performance of the proposed FedRME compared with the benchmarks of centralized learning and standalone learning.

A. Simulation setups

1) Wireless environment: The target area is a square with a side length 48m and is discretized into a 48×48 grid. For FedRME and standalone methods, the target area is partitioned with $N_x = N_y = 3$, resulting 9 patches of radiomap with dimension 16×16, each estimated by a distributed fusion center. To analyze the most fundamental cartographic aspects, we set $\mathcal{F}$ to the singleton $\mathcal{F} = \{1400\text{MHz}\}$ and bandwidth to 5MHz. The training and testing data are generated using the ray tracing algorithm provided by Remcom's Wireless Insite software in the "urban canyon" scenario [9]. This algorithm is based on the shooting and bouncing ray method [20], with the maximum number of reflections and diffractions set to 6 and 2, respectively. A binary mask indicating the position of obstacles is used in the data as the landscape map. In each ground truth radiomap, one transmitter with a height of 1.5m is deployed. The transmit power of each transmitter is randomly chosen between 5 and 11 dBm. The noise $\upsilon(i, j, f)$ is randomly chosen between -180 and -170dBm/MHz. Based on previous studies, the input measurements and the label for the radiomap, i.e., $\tilde{\mathbf{\Psi}}$ and $\hat{\mathbf{\Psi}}$, are expressed in logarithmic unit dBm [9].

2) Model configurations: As shown in Fig. 2, each type of convolutional autoencoder in this paper has 3 modules in the encoder and the decoder, respectively. Each module consists of 3 convolutional or deconvolutional layers followed by an average pooling or up-sampling layer. All convolutional or deconvolutional layers in the modules share the same kernel size of 3×3 and the stride of 1. The average pooling layers in the encoder have the size of 2×2 and the stride of 2. The up-sampling layers in the decoder share an up-sampling factor of 2. For the centralized autoencoder whose input data corresponds to all 48×48 grids of the whole area, we set the number of neurons of the convolutional or deconvolutional layers in all modules to 27 and set the code length of the latent variable to 72. For the distributed autoencoders in the FedRME and standalone learning, we set the expanding depth $d = 4$ such that the input/output of distributed autoencoders covers 24×24 grids. Considering the reduced complexity in the distributed methods, we reduce the neuron numbers per layer in their modules to 13 and set the code length of their latent variables to 36.

3) DNN complexity: The autoencoder DNN for the centralized method has 100101 parameters which take up about 391KB. Each autoencoder for the distributed methods has 25481 parameters, which occupies only 100KB. By using the proposed federated learning approach, the model complexity of each fusion center is reduced by about 75%.

4) Training scheme: We use the ADAM [21] optimizer for all methods with training batch size 32 and set the learning rates for all methods to 1×10^{-4}. To improve the stability of federated learning, we apply gradient clipping to the distributed autoencoders such that the global norm of gradients during local training is no larger than 1000. For the proposed federated learning, the distributed fusion centers average their autoencoder parameters once per local training epoch. The standalone method is trained with local data, but without model averaging. All methods are trained for sufficient epochs until convergence. The learning capability of each method is evaluated under two cases with different training data volumes. In Case 1, there is a relatively large training dataset that contains 20000 radiomaps. For Case 2, there are only 1000 radiomaps for training, which simulates the scenarios with data scarcity. The number of sensors per map in the training data, N, is uniformly and randomly selected between 1% and 20% of the total number of grid points ($N \in [24, 461]$). In this way, autoencoders can be trained to handle RME tasks with varying numbers of sensors.

B. Results and discussions

We compare our proposed FedRME with the benchmarks by evaluating their estimation accuracy and visualizing their outputs. The estimation accuracy is measured by the RMSE averaged over 1000 testing data.

1) Case 1-Sufficient training data: We train different methods in Case 1 and test the average RMSE of these methods under a range of sensor numbers $N \in [70, 500]$. As shown in Fig. 3, the proposed method performs nearly as good as the centralized method except when N gets small, while greatly outperforming the standalone learning. These results demonstrate that the federated learning method has outstanding learning capability compared with standalone learning.

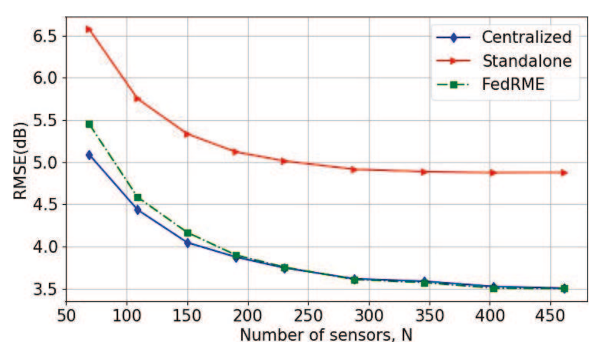

Fig. 3. RMSE of different methods trained on a big dataset.

2) Case 2-Small training data: We train these methods under Case 2 and test their average RMSE in the same range of sensor numbers. As depicted in Fig. 4, the proposed FedRME achieves the lowest estimation error under all sensor numbers in the range. This indicates that our method is the most effective in learning from insufficient data and is the most robust against overfitting. The centralized method achieves a better RMSE than the standalone method, this means the large centralized autoencoder has high learning capability but it is highly degraded by overfitting. The standalone method achieves the worst performance, considering that it shares the same local data and autoencoder design as our method, this demonstrates the proposed federated learning method plays a more impactful role than the compact DNN design itself.

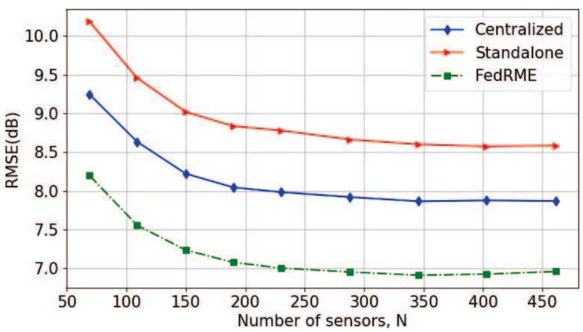

Fig. 4. RMSE of different methods trained on a small dataset.

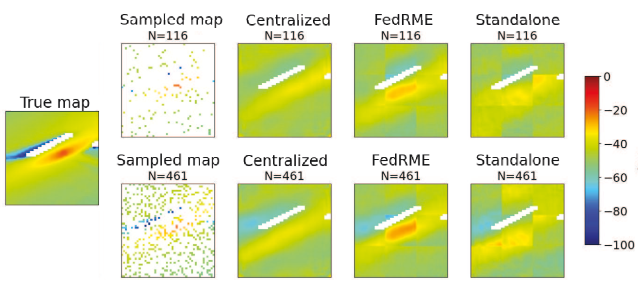

Fig. 5. Radiomaps estimated with different methods given 2 groups of sensor numbers: $\{116, 461\}$, where white areas represent buildings.

We also visualize an example of the true radiomap, the incomplete spectrum measurements with 2 groups of sensor numbers $N \in \{116, 461\}$, and the corresponding outputs generated by different methods in case 2. As shown in Fig. 5, the proposed method makes the most accurate estimation of the transmitter. By contrast, the centralized method fails to find the transmitter, which may be the consequence of overfitting. The standalone learning method shows the worst continuity across adjacent patches and estimates too many sources, which is a sign of inferior learning capability.

V. Conclusions

This paper develops a novel federated learning framework with distributed fusion centers for radiomap estimation. By leveraging federated learning, we enhance the learning capability of distributed compact autoencoders and improve robustness against overfitting despite limited training data. Simulation results verify that FedRME achieves a better trade-off between estimating accuracy and computation efficiency.

References

[1] S. Grimoud, S. B. Jemaa, B. Sayrac, and E. Moulines, "A rem enabled soft frequency reuse scheme," in *2010 IEEE Globecom Workshops*. IEEE, 2010, pp. 819–823.

[2] B. A. Jayawickrama, E. Dutkiewicz, I. Oppermann, G. Fang, and J. Ding, "Improved performance of spectrum cartography based on compressive sensing in cognitive radio networks," in *2013 IEEE International Conference on Communications (ICC)*. IEEE, 2013, pp. 5657–5661.

[3] A. B. H. Alaya-Feki, S. B. Jemaa, B. Sayrac, P. Houze, and E. Moulines, "Informed spectrum usage in cognitive radio networks: Interference cartography," in *2008 IEEE 19th International Symposium on Personal, Indoor and Mobile Radio Communications*. IEEE, 2008, pp. 1–5.

[4] S.-J. Kim and G. B. Giannakis, "Cognitive radio spectrum prediction using dictionary learning," in *2013 IEEE Global Communications Conference (GLOBECOM)*. IEEE, 2013, pp. 3206–3211.

[5] G. Ding, J. Wang, Q. Wu, Y.-D. Yao, F. Song, and T. A. Tsiftsis, "Cellular-base-station-assisted device-to-device communications in tv white space," *IEEE Journal on Selected Areas in Communications*, vol. 34, no. 1, pp. 107–121, 2015.

[6] D.-H. Huang, S.-H. Wu, W.-R. Wu, and P.-H. Wang, "Cooperative radio source positioning and power map reconstruction: A sparse bayesian learning approach," *IEEE Transactions on Vehicular Technology*, vol. 64, no. 6, pp. 2318–2332, 2014.

[7] Y. Teganya and D. Romero, "Data-driven spectrum cartography via deep completion autoencoders," in *IEEE International Conference on Communications (ICC)*. IEEE, 2020, pp. 1–7.

[8] D. Romero and S.-J. Kim, "Radio map estimation: A data-driven approach to spectrum cartography," *IEEE Signal Processing Magazine*, vol. 39, no. 6, pp. 53–72, 2022.

[9] Y. Teganya and D. Romero, "Deep completion autoencoders for radio map estimation," *IEEE Transactions on Wireless Communications*, vol. 21, no. 3, pp. 1710–1724, 2021.

[10] S. Shrestha, X. Fu, and M. Hong, "Deep generative model learning for blind spectrum cartography with nmf-based radio map disaggregation," in *ICASSP 2021-2021 IEEE International Conference on Acoustics, Speech and Signal Processing (ICASSP)*. IEEE, 2021, pp. 4920–4924.

[11] S. Zhang, A. Wijesinghe, and Z. Ding, "Rme-gan: A learning framework for radio map estimation based on conditional generative adversarial network," *IEEE IoT-J*, vol. 10, no. 20, pp. 18 016–18 027, 2023.

[12] S. Zhang, T. Yu, B. Choi, F. Ouyang, and Z. Ding, "Radiomap inpainting for restricted areas based on propagation priority and depth map," *IEEE Transactions on Wireless Communications*, 2024.

[13] R. Levie, Ç. Yapar, G. Kutyniok, and G. Caire, "Radiounet: Fast radio map estimation with convolutional neural networks," *IEEE Transactions on Wireless Communications*, vol. 20, no. 6, pp. 4001–4015, 2021.

[14] S. Zhang, B. Choi, F. Ouyang, and Z. Ding, "Physics-inspired machine learning for radiomap estimation: Integration of radio propagation models and artificial intelligence," *IEEE communications magazine*, 2024.

[15] B. McMahan, E. Moore, D. Ramage, S. Hampson, and B. A. y Arcas, "Communication-efficient learning of deep networks from decentralized data," in *Artificial Intelligence and Statistics*. PMLR, 2017, pp. 1273–1282.

[16] S. Iizuka, E. Simo-Serra, and H. Ishikawa, "Globally and locally consistent image completion," *ACM Transactions on Graphics (ToG)*, vol. 36, no. 4, pp. 1–14, 2017.

[17] T. Imai, K. Kitao, and M. Inomata, "Radio propagation prediction model using convolutional neural networks by deep learning," in *2019 13th European Conference on Antennas and Propagation (EuCAP)*. IEEE, 2019, pp. 1–5.

[18] M. Iwasaki, T. Nishio, M. Morikura, and K. Yamamoto, "Transfer learning-based received power prediction with ray-tracing simulation and small amount of measurement data," in *2020 IEEE 92nd Vehicular Technology Conference (VTC2020-Fall)*. IEEE, 2020, pp. 1–6.

[19] I. Goodfellow, Y. Bengio, and A. Courville, *Deep learning*. MIT press, 2016.

[20] H. Ling, R.-C. Chou, and S.-W. Lee, "Shooting and bouncing rays: Calculating the rcs of an arbitrarily shaped cavity," *IEEE Transactions on Antennas and propagation*, vol. 37, no. 2, pp. 194–205, 1989.

[21] D. P. Kingma and J. Ba, "Adam: A method for stochastic optimization," *arXiv preprint arXiv:1412.6980*, 2014.